Paper

Numerical Evaluation of Electromagnetic-wave Penetration at Normal Incidence through an Inhomogeneous-wave Approach

Alessandro Calcaterra[1], Fabrizio Frezza[1], Patrizio Simeoni[2], and Nicola Tedeschi[1]

[1] *Department of Information Engineering, Electronics and Telecommunications, La Sapienza University of Rome, Rome, Italy*
[2] *National Transport Authority (NTA), Dublin, Ireland*

https://doi.org/10.26636/jtit.2018.124218

Abstract— This paper presents numerical scenarios concerning penetration in a lossy medium that can be obtained by radiating inhomogeneous electromagnetic waves. Former papers approached this problem, both analytically and numerically, finding requirements and limits of the so-called "deep-penetration" condition, which consists of a wave transmitted in a lossy medium having an attenuation vector whose direction forms the angle of ninety degrees with the normal to the separation surface. The deep-penetration condition always requires an oblique incidence, therefore is not practical in many applications. For this reason, we are interested here in finding whether an inhomogeneous wave guarantees larger penetration than the one obtainable with homogeneous waves, even when the incident wave is normal to the separation surface between two media, i.e. when the deep-penetration condition is not satisfied. We are also interested in verifying numerically whether the lossy-prism structure may achieve larger penetration than the one obtainable through traditional leaky-wave antennas, and we also wish to propose a lossy-prism design more realistic than the one previously presented in the literature.

Keywords—deep-penetration, electromagnetic simulation, leaky-wave antennas, lossy prism.

1. The Scenario

In this article, we study a typical near-field problem, in which antennas generate electromagnetic radiation that propagates first in the air, for a short distance (near-field), here approximated by a vacuum, and then impinges normally to the separation surface with a lossy medium. Such a problem represents a typical air-coupled antenna scenario. In [1], [2], authors found analytical requirements and restrictions of the so-called "deep-penetration" condition. The problem studied in such papers is the incidence of an inhomogeneous plane wave, incoming from a lossless medium, on a planar and infinite separation surface with a lossy medium. Those papers found conditions in which the transmitted wave generated in the lossy medium attenuates along the interface – this guarantees infinite penetration. In realistic scenarios, i.e. when the electromagnetic field is generated by a finite source, the deep-penetration condition can only be supported in a limited spatial region. It was observed that leaky-wave antennas [3], [4] can be employed to generate an electromagnetic field suitable for deep penetration in near-field [5].

Moreover, it was demonstrated in [1], [2], that the deep-penetration condition can only be obtained for oblique incidence. Such a condition, as highlighted in [6], is not very practical for many applications, where, instead, normal incidence is recommended. We investigate here the penetration achievable in the normal incidence condition employing leaky-wave antennas, we numerically verify the role played by the incidence angle, and finally, the lossy prism proposed in [6] is numerically studied in a suitable antenna structure to verify its penetration properties. The design proposed here is a numerical prototype which intends to serve as an input to lossy-prism antennas design for practical and realistic scenarios.

2. Normal Incidence of Inhomogeneous and Homogeneous Plane Waves

In Fig. 1, the incidence of an inhomogeneous wave on a separation surface between a lossless and a lossy medium is illustrated: $\boldsymbol{\beta}_1$ represents the phase vector of the incident wave, $\boldsymbol{\alpha}_1$ the attenuation vector of the incident wave, $\boldsymbol{\beta}_2$ the phase vector of the transmitted wave, and finally $\boldsymbol{\alpha}_2$ the attenuation vector of the transmitted wave. ξ_1 is the angle of incidence, and the angles formed by $\boldsymbol{\beta}_2$ and $\boldsymbol{\alpha}_2$ with the normal to the separation surface are defined as ξ_2 and ζ_2, respectively. In the lossy medium region, the amplitude α_2 of the vector $\boldsymbol{\alpha}_2$ needs to be always different from zero, but the ζ_2 angle can assume different values.

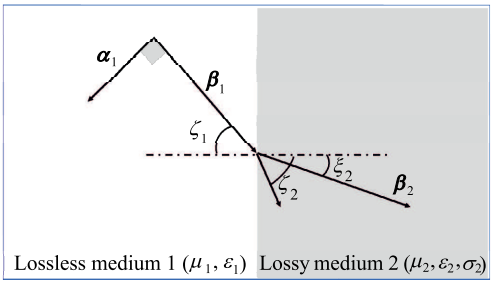

Fig. 1. Theoretical geometry of the problem: an incident inhomogeneous-plane wave characterized by a phase vector $\boldsymbol{\beta}_1$ and an attenuation vector $\boldsymbol{\alpha}_1$ is generated in a lossless medium and it impinges on an infinite and planar separation surface with a lossy medium generating a transmitted wave whose phase vector is indicated by $\boldsymbol{\beta}_2$ and attenuation vector is indicated with $\boldsymbol{\alpha}_2$.

The tangential component of the electromagnetic field is conserved at the interface between two media [7]. It follows that, in the case of an incident homogeneous wave ($\boldsymbol{\alpha}_1 = 0$), $\zeta_2 = 0$. When the incident wave is inhomogeneous, in turn, it must necessarily be $\zeta_2 > 0$ [7].

It is therefore reasonable to expect that, even when $\xi_1 = 0$ in Fig. 1, the penetration obtained through inhomogeneous waves needs to be larger than the one that can be obtained by employing a homogeneous incident wave, simply because the presence of a $\zeta_2 > 0$ angle results in a transmitted wave which does not attenuate in the direction orthogonal to the separation surface. To demonstrate this, let us impose $\xi_1 = 0$ and let us define with $\hat{\mathbf{x}}$ and $\hat{\mathbf{z}}$ the unit vectors parallel and perpendicular to the separation interface, respectively. We can write:

$$\begin{aligned} \boldsymbol{\alpha}_2 &= \alpha_{2t}\hat{\mathbf{x}} + \alpha_{2n}\hat{\mathbf{z}} \\ \boldsymbol{\beta}_2 &= \beta_2\hat{\mathbf{z}} \end{aligned}. \tag{1}$$

Let us now define with $\mathbf{k}_2$ the wave vector of the transmitted wave, with $\mathbf{k}_1$ the wave vector of the incident wave, and with k_2 the amplitude of $\mathbf{k}_2$. It is [7]:

$$\begin{aligned} \mathbf{k}_2 &= \boldsymbol{\beta}_2 - \mathrm{j}\boldsymbol{\alpha}_2 \\ \mathbf{k}_1 &= \boldsymbol{\beta}_1 - \mathrm{j}\boldsymbol{\alpha}_1 \end{aligned}. \tag{2}$$

From Eqs. (1)–(2):

$$\begin{aligned} \beta_2^2 &= \mathrm{Re}^2 k_2 + \alpha_{2t}^2 + \alpha_{2n}^2 \\ \beta_2\alpha_{2n} &= \mathrm{Im}\, k_2 \end{aligned} \tag{3}$$

Therefore:

$$\beta_2^4 - \left(\mathrm{Re}^2 k_2 + \alpha_{2t}^2\right)\beta_2^2 - \mathrm{Im}^2 k_2 = 0\,. \tag{4}$$

Taking twice the positive sign, β can be found from the bi-quadratic Eq. (4):

$$\beta_2 = \frac{1}{\sqrt{2}}\sqrt{\mathrm{Re}^2 k_2 + \alpha_{2t}^2 + \sqrt{\left(\mathrm{Re}^2 k_2 + \alpha_{2t}^2\right)^2 + 4\,\mathrm{Im}^2 k_2}}\,. \tag{5}$$

At a given frequency, k_2 depends only on the medium [7], therefore it does not change modifying ξ_1. But then, from Eq. (5), we can see that the larger α_{2t} is, the larger β_2 becomes, and consequently, from the second equation in (3), α_{2n} needs to get smaller. Therefore, the penetration-depth increases. The minimum value of β_2 is obtained when $\alpha_{2t} = 0$, i.e. in the case of an impinging homogeneous wave, as expected.

The demonstration presented in this section is purely mathematical, we need to choose an appropriate physical inhomogeneous wave to validate the finding.

In [8], different kinds of inhomogeneous waves are studied, and it is shown that the leaky wave is the only one which is not bound to the separation surface between a lossless and a lossy medium. This waveform is the most suitable for our exploration, because it can be locally approximated by an inhomogeneous plane wave. Moreover, such a waveform can be easily generated through well-known structures named leaky-wave antennas [3], [4].

Unfortunately, as written earlier, such a wave can be supported only for a limited distance from the antenna aperture. This constraint limits the advantage in terms of penetration that can be obtained employing those structures over the one achievable through more traditional antenna design (e.g. horns).

3. The Two-dimensional Leaky-wave Antenna

The first objective of this paper is to extend, and complete, the study presented in [9] related to the penetration that can be obtained employing the two-dimensional planar antenna designed in [10]. This antenna is, in principle, equivalent to the substrate-superstrate leaky-wave antenna (see [11], [12]) as demonstrated in [13], but it does not present the disadvantage of a high-permittivity layer. Two-dimensional and periodic leaky-wave antennas have the advantage of creating a pencil beam at broadside, which is the direction of interest here, employing a very simple feeder. A mono-dimensional and periodic antenna could also represent a suitable solution because, even though those structures present a natural stop-band at broadside [3], [4], examples are present in literature of projects that can guarantee broadside radiation employing those structures [14], [15]. Anyway, the mono-dimensional periodic LWAs still require challenging design for achieving the stop-band suppression at broadside.

For all reasons exposed above, the two-dimensional and periodic leaky-wave antenna was selected for some preliminary promising qualitative results in terms of penetration depth, in [9].

The antenna is designed to radiate at 12 GHz, mainly to allow an easy comparison with former inhomogeneous-wave penetration studies, such as [5] and [9], where such a frequency was chosen. The antenna, which is assumed of infinite dimension in [10], was modelled on CST Microwave

Studio Software [16] (see Fig. 18) using a structure of 22×12 patches according to the geometry illustrated in Fig. 2, where patch and periodicity dimensions are also listed, such dimensions are chosen in agreement with the values suggested in [9] and [10]. Rogers RT5870 was chosen as the medium for the substrate (relative permittivity $\varepsilon_r = 2.33$, relative permeability $\mu_r = 0$), and losses in the substrate were neglected. The thickness of the substrate

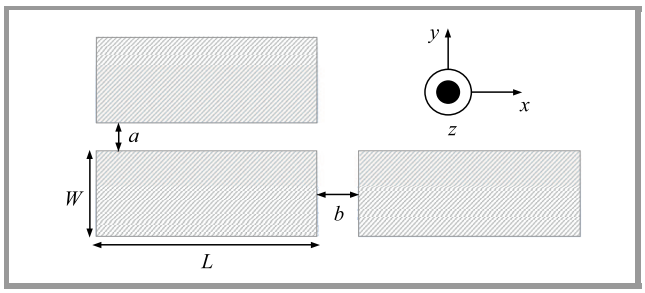

Fig. 2. Patch structure of the two-dimensional leaky-wave antenna: $L = 11$ mm, $W = 3$ mm, $b = 2$ mm, and $a = 1$ mm. Metal patches were designed assuming PEC as a material to speed-up the simulation.

in this antenna controls the beam direction for a given frequency [10], [17], i.e. for the n-th mode, it is (Eq. (2) in [10]):

$$h_s = \lambda_0 \cdot \frac{n}{2\sqrt{\varepsilon_r - \sin^2 \theta_p}}, \tag{6}$$

where θ_p is the scanning angle. Having chosen the $n = 1$ radiation mode, from $\varepsilon_r = 2.33$, and from the operating frequency of 12 GHz, it follows:

$$h_s = 0.025 \cdot \frac{1}{2\sqrt{2.33}} \approx 0.0082 \text{ m}. \tag{7}$$

The value indicated by Eq. (7) was modified into $h_s = 8.40$ mm after having run the parameter sweep option of CST on the beam direction.

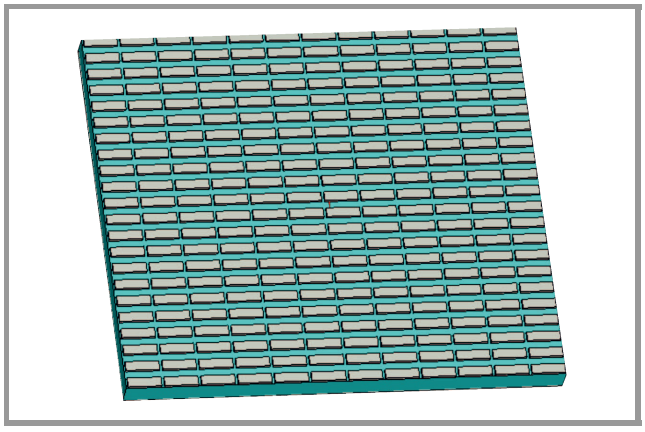

Fig. 3. Two-dimensional leaky-wave antenna design on CST Microwave Studio. (See color pictures online at www.nit.eu/publications/journal-jtit)

The radiation pattern on the E-plane generated by this leaky-wave antenna is shown in Fig. 4, while the radiation pattern for the H-plane is shown in Fig. 5.

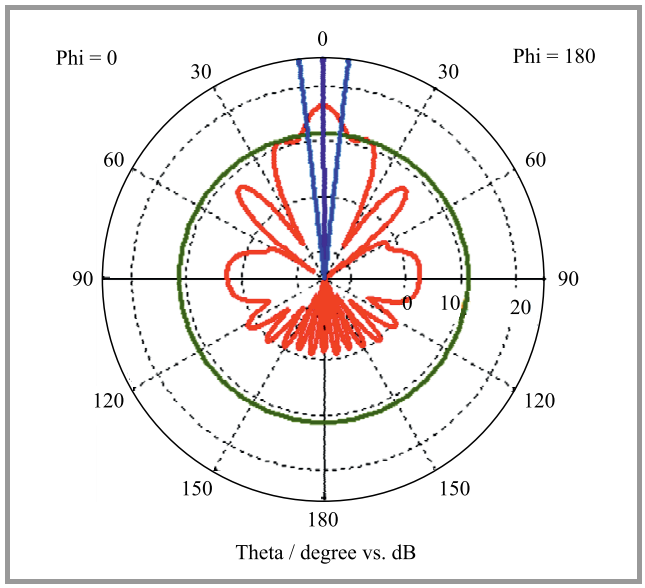

Fig. 4. Broadside radiation pattern on the E-plane.

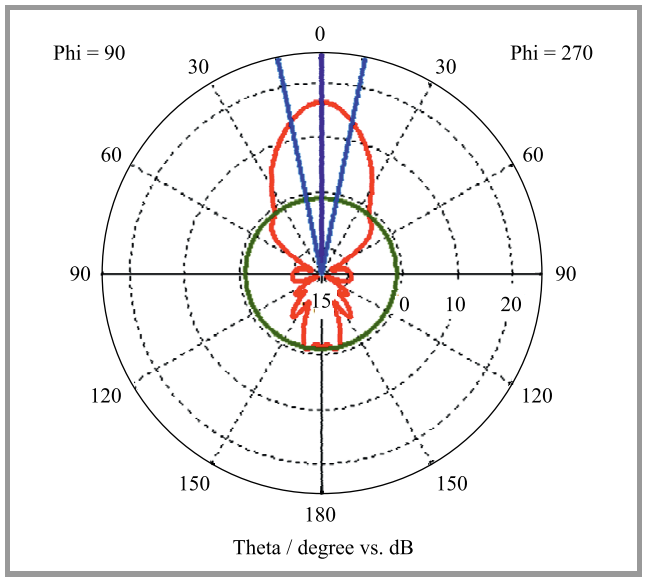

Fig. 5. Broadside radiation pattern on the H-plane.

The E-plane has grating lobes due to the presence of the surface wave which is mostly directed on such a plane, in perfect agreement with the behavior exposed in [10] and [17]. The antenna was fed by a $\frac{1}{2}\lambda$ horizontal dipole placed at a distance $h_d = 0.5h_s$ from the antenna ground plane. The dipole does not represent a practical, realistic feeding, but it can be replaced, for instance, by a microstrip slot [18] on a hypothetical prototype.

To compare the penetration produced by this antenna with the one produced by more commonly used antennas, a lossy medium, characterized by a conductivity $\sigma = 0.05$ S/m, unitary relative permittivity and unitary relative permeabil-

ity was designed and positioned at a distance $d = \frac{3}{2}\lambda$ from the antenna aperture, as shown in Fig. 6. The choice of a unitary relative permittivity for the lossy medium is fundamental to avoid the influence of the incidence angle on the penetration. A relative permittivity $\varepsilon_r = 1$ and a low enough value of conductivity σ, such as the value chosen, allow to neglect reflections independently of the incidence angle: such a choice permits to compare antennas radiating at different angles. Different choices for the lossy medium could potentially complicate the comparison because the behavior in terms of penetration could strongly depend on the incidence angle (e.g. pseudo-Brewster angle or total transmission [19]). Moreover, $\varepsilon_r = 1$ and $\sigma = 0.05$ S/m were assumed in previous deep-penetration studies (see for instance [9]), therefore the choice made here allows a direct comparison with the literature.

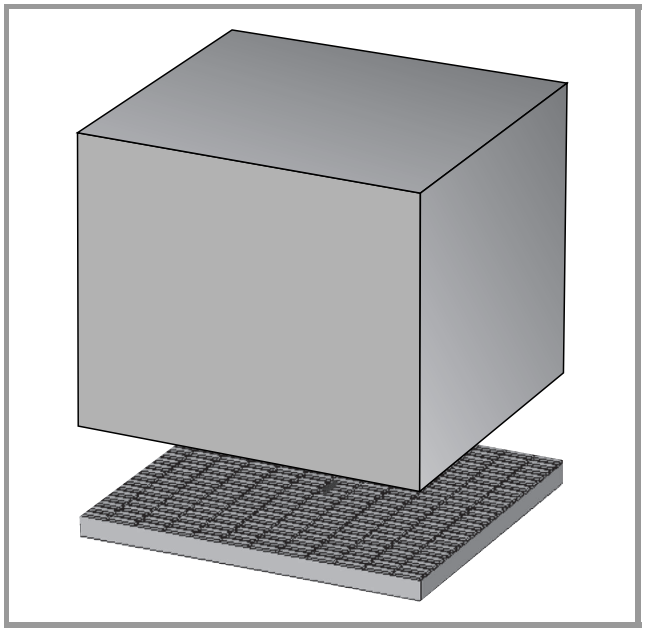

Fig. 6. Lossy medium positioned above the antenna aperture: note that the lossy medium base is chosen as large as the aperture, to avoid radiation entering from the lateral faces of the lossy prism.

The distance $d = \frac{3}{2}\lambda$ was chosen in accordance with the criteria that request the lossy medium to be inside the radiating near-field region [5].

4. Homogeneous-wave Antennas

Pyramidal- and circular-horn antennas were designed to act as a comparison for the penetration achieved by the two-dimensional periodic leaky-wave antenna. An almost omnidirectional antenna, and in particular a $\frac{1}{2}\lambda$ dipole [20], was also simulated to serve as reference for the minimum achievable penetration. All mentioned antennas were optimized to radiate at a frequency of 12 GHz, because a direct penetration comparison is possible only when both frequencies and lossy media are equivalent.

4.1. Circular-horn Antenna

The circular-horn antenna was designed following the procedure illustrated in [21]. The radius of the aperture resulted $r_c = 25.4$ mm. Perfect Electric Conductor (PEC) was chosen as metal for the structure, to increase the simulation speed, and the antenna was fed by means of a waveguide port. The amplitude of the scattering reflection coefficient at the first port (S_{11}) is illustrated in Fig. 7.

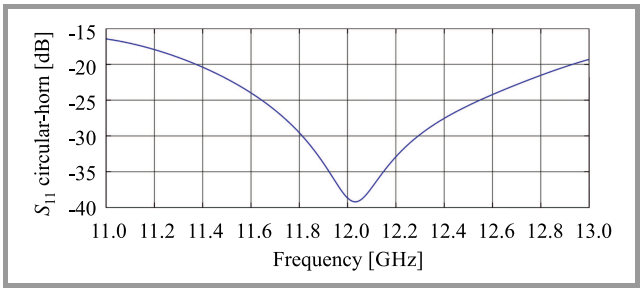

Fig. 7. Amplitude of the S_{11} scattering parameter for the circular-horn antenna, the resonance at $f_0 = 12$ GHz is visible.

A lossy medium equivalent to the one used for the periodic two-dimensional LWA was posed, again, at a distance $d = \frac{3}{2}\lambda$ from the antenna aperture. The CST design of the structure is shown in Fig. 8.

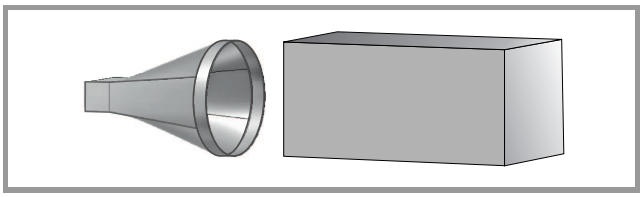

Fig. 8. Design of the circular-horn antenna with a lossy medium posed at a distance $d = \frac{3}{2}\lambda$ from the antenna aperture, note that the lossy prism base is as large as the antenna aperture to guarantee the infinite planar separation surface approximation in near-field condition.

4.2. Pyramidal-horn Antenna

The pyramidal-horn antenna was designed having aperture dimensions of 107.8×137.4 mm. The metal for the horn antenna enclosure was approximated with a PEC, and the antenna was fed by means of a waveguide port. The amplitude of the S_{11} scattering parameter for this antenna is shown in Fig. 9.
A lossy medium equivalent to the one used for the periodic two-dimensional LWA was posed, again, at a distance $d = \frac{3}{2}\lambda$ from the antenna aperture. The CST design of the structure is shown in Fig. 10.

4.3. Dipole Antenna

A 0.5λ dipole antenna was also designed. Obviously such an antenna is not expected to have high performance in terms of penetration, but it was designed to act as a reference, so that the improvement in penetration introduced by

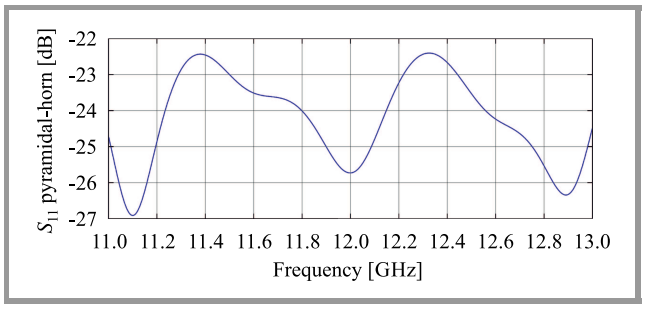

Fig. 9. Amplitude of the S_{11} scattering parameter for the pyramidal-horn antenna, this antenna presents clear broadband characteristics.

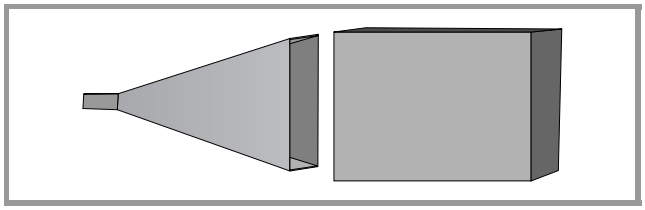

Fig. 10. Design of the pyramidal-horn antenna with a lossy medium posed at a distance $d = \frac{3}{2}\lambda$ from the antenna aperture, note that the lossy prism base is as large as the antenna aperture to guarantee the infinite planar separation surface approximation in near-field condition.

the LWA with respect to the horn antenna could be compared against the improvement that the horn antenna would introduce with respect to a non-directive antenna, such as the dipole chosen. The dipole arms were assumed PEC, again, and the dipole was fed by a discrete port between the arms, as shown in Fig. 11.

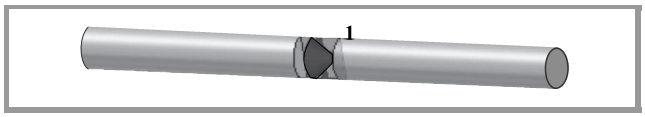

Fig. 11. Design of a $\frac{1}{2}\lambda$ dipole antenna, fed by a discrete port.

5. Simulation Results

5.1. Penetration Comparison

Let us assume, without loss of generality, the direction of the maximum amplitude of the electric field, which for the designed antennas corresponds to the direction normal to both antenna aperture and interface with the lossy medium, along the z axis. To compare the penetration achieved by the antennas illustrated in the previous paragraph, the amplitude of the electric field $|\mathbf{E}|$ was first evaluated using the E-field monitor option of CST Microwave Studio for all the antennas, then results were exported to Matlab for further processing. In Matlab, the value of the field at the separation interface with the lossy medium: $E_{\text{if}}^{\text{MAX}} = |\mathbf{E}(0,0,1.5\lambda)|$ was extracted first. Then, every sample of the field, such that $E_z = |\mathbf{E}(0,0,z)|$, where $z > \frac{3}{2}\lambda$ was normalized by such a value. The normalized electric field curve obtained is therefore:

$$|\mathbf{E}_{\text{zn}}| = \frac{|\mathbf{E}(0,0,z)|}{E_{\text{if}}^{\text{MAX}}}, \text{where } z > \frac{3}{2}\lambda\,. \tag{8}$$

We evaluated this normalized curve for all antennas: the results are presented in Fig. 12. The curve for the planar two-dimensional LWA presents a higher penetration in the lossy medium. However, as expected, the slope of the curve is always negative, even at the interface. This is due to a low amplitude of propagation and attenuation vectors which must result in $\zeta_2 < 90°$. A second, important result, is that the best performances for the homogeneous wave generators are obtained through the pyramidal antenna. By visual inspection it is also possible to verify that the advantage introduced by the LWA on the pyramidal horn is comparable with the one that the pyramidal horn has on the dipole, at least up to approximately 60 mm inside the lossy medium, i.e. $\frac{12}{5}\lambda$.

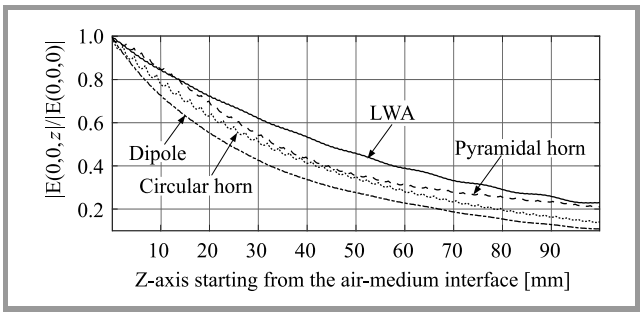

Fig. 12. Comparison between electric-field amplitudes produced by various antennas and propagating inside a lossy non-magnetic medium, of relative permittivity $\varepsilon_r = 1$ and conductivity $\sigma = 0.05$ S/m; the fields are evaluated as described by Eq. (8).

5.2. Results Varying the Conductivity

In [1] and [2], the deep-penetration condition is verified from an analytical-theoretical point of view, and in [5] preliminary results demonstrate that the deep-penetration condition can be met employing simple uniform leaky-wave structures such as the Menzel antenna [22], [23].
In [5], the field generated by the Menzel antenna is studied for different values of the lossy-medium conductivity σ, but no comparison is performed with other antennas. Here, instead, simulations are performed to compare the difference of electric-field penetration between the pyramidal-horn antenna and the two-dimensional LWA through:

$$f(z) = E^{\text{LWA}}(0,0,z) - E^{\text{HORN}}(0,0,z)\,, \tag{9}$$

where $E^{\text{LWA}}(0,0,z)$ and $E^{\text{HORN}}(0,0,z)$ represent the normalized electric fields inside the lossy medium for the LWA and pyramidal-horn antenna, respectively – Eq. (8). Equation (9) is evaluated for different values of conductivity σ of the lossy medium, while its relative permittivity and permeability are kept constant ($\varepsilon_r = 1$ and $\mu_r = 1$). Other antennas, mentioned in the previous paragraph, were not

considered in this comparison because they provide lower penetration than the one achievable by the pyramidal horn, see Fig. 12. The result is given in Fig. 13, where every curve represents the difference between the amplitudes of the electric fields, normalized as in Eq. (8), produced by the LWA and the horn antennas, respectively, for a specific conductivity value of the lossy medium. We can observe that increasing the σ value of the lossy medium the penetration performance of the two antennas tends to align, while when σ diminishes LWA penetration becomes noticeably higher.

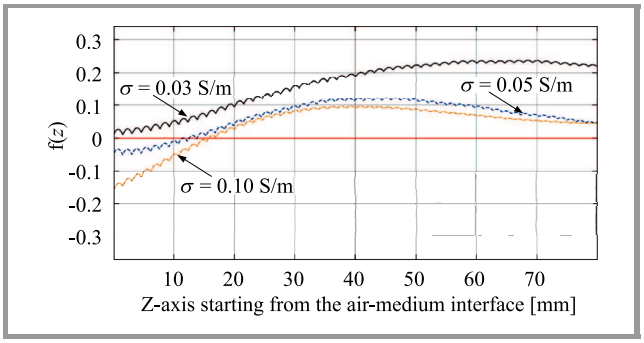

Fig. 13. Difference between normalized electric-field amplitudes generated by a planar leaky-wave antenna and a pyramidal-horn antenna inside the medium computed according to Eq. (9). Curves are shown for conductivity values of $\sigma = 0.03$ S/m, $\sigma = 0.05$ S/m, and $\sigma = 0.1$ S/m. Relative permittivity and permeability are $\varepsilon_r = 1$ and $\mu_r = 1$, respectively.

This result confirms the theoretical results found in [6] for inhomogeneous plane waves.

5.3. Results Varying the Incident Angle

Finally, it was important to verify the property demonstrated for plane waves in [1], [2] for which a larger incidence angle would result in a deeper penetration in a lossy medium through inhomogeneous waves. As the two-dimensional patch LWA presents a very low amplitude of the attenuation vector $\boldsymbol{\alpha}$, it follows that the best penetration condition is guaranteed by an incidence angle $\xi_1 = 45°$. Anyway, such an angle cannot easily be exploited with the designed antenna for the presence of the -1 space harmonic of TM_0 surface wave [10], whose perturbation effect, mainly on the E-plane, is larger for larger values of the scanning angle. It is not possible to increase the incidence angle by rotating either the antenna or the lossy medium, because doing so could cause the lossy medium to enter inside the reactive near-field zone. This would change the nature of the problem that is studied here. For the LWA analyzed here, the effects of the surface wave were considered negligible when $\xi_1 \leq 30°$, therefore $\xi_1 = 30°$ was chosen as the maximum value for the incidence angle. Leaky-wave antennas perform a frequency scan, but here, we needed to compare the penetration at different angles without varying the frequency. Therefore, we had to re-design the antenna increasing the substrate thickness. From Eq. (6), it follows that $h_s = 8.7$ mm: $h_s = 8.9$ mm was chosen after the parameter-sweep optimization in CST. We needed to guarantee that the second order mode would not appear at broadside when the first mode reaches the angle of 30°. This requirement translates into a minimum value for the relative permittivity, which can be evaluated imposing Eq. (6) for both $n = 1$ and $n = 2$ modes, and comparing the two (see Eq. (5) of [10]), obtaining the:

$$\varepsilon_r > \frac{4}{3}\sin^2\theta_p\,. \tag{10}$$

In particular $\varepsilon_r > 1/3$ is required for the antenna designed here. The permittivity value chosen in this paper ($\varepsilon_r = 1$) respects this condition, and therefore guarantees the absence of higher-order modes at the desired angle. It is clear that the chosen amplitude for the substrate permittivity would guarantee the absence of the second order mode even when the $n = 1$ mode would be at endfire ($\varepsilon_r > 4/3$, i.e. the case illustrated in Eq. (5) of [10]).
The result of the investigation is shown in Fig. 14. The penetration obtained by the oblique beam at 30° is slightly larger than the one obtained by broadside radiation, as expected according to the theoretical results found in [1], [2].

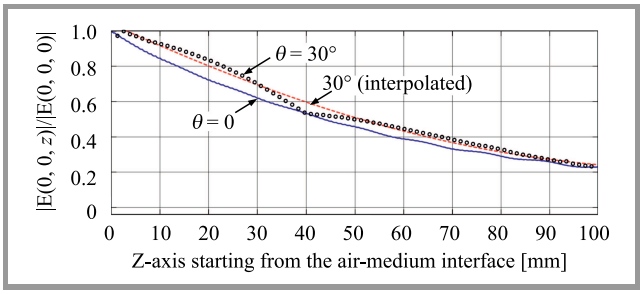

Fig. 14. Normalized electric field amplitude inside the lossy medium – Eq. (8) for broadside radiation ($\xi_1 = 0°$) and for $\xi_1 = 30°$. The lossy medium has conductivity $\sigma = 0.05$ S/m and relative permittivity $\varepsilon_r = 1$. The field is generated by the two-dimensional periodic LWA at a frequency of 12 GHz.

6. Leaky Wave Through a Two-dimensional Lossy Prism

Recently, it has been demonstrated, analytically, that a two-dimensional lossy prism, firstly introduced in [24], may achieve a larger penetration than the one obtained by conventional leaky-wave antennas [6]. The first numerical prototype of this geometrical structure was presented in [25]. In that paper, the prism was illuminated by the far-field generated by a customary horn antenna. Such a setup cannot easily lead to a suitable antenna design, so we analyze here an alternative, and more practical, feeding structure. We propose to position the lossy prism at the aperture of a TEM-horn antenna, i.e. a two-dimensional horn antenna also known in the literature as dihedral horn [26]: a TEM antenna allows a full control of the beam incidence angle on the lossy prism. The vertex of the lossy prism, indicated

with χ in [6], is set to 90°, as suggested in [6]. It makes sense to verify whether the electromagnetic field can penetrate more deeply inside the lossy medium in this case, where the illumination is not exactly a plane wave, as it was, instead, in [6]. The proposed structure was designed in Comsol Multiphysics, and it is illustrated in Fig. 15.

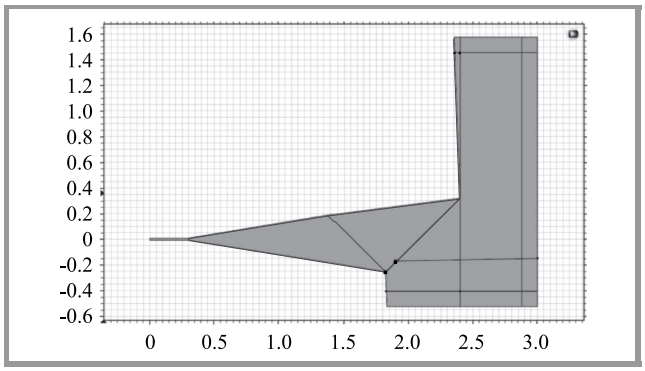

Fig. 15. Comsol simulation of a two-dimensional TEM-horn antenna having a lossy prism attached to the aperture.

The lossy prism was chosen to be of the non-magnetic kind and having a relative complex permittivity of $\varepsilon_r = 1 - \mathrm{j}0.05$. The two-dimensional horn antenna radiates at a frequency of 12 GHz. At such a frequency, the conductivity of the prism is $\sigma = 0.005$ S/m. It is possible to obtain the amplitudes of attenuation vector α_3, and phase vector β_3 of the generated inhomogeneous wave using the formulas presented in [6], which are reported here for the case of interest:

$$\begin{aligned} k_0 &= \omega\sqrt{\mu_0\varepsilon_0} = 252.167972 \text{ rad/m} \quad , \\ \beta_3 &= \frac{k_0}{\sqrt{2}}\sqrt{1+\sqrt{1+\left(\frac{2\varepsilon''_{r2}}{\sin(2\xi_3)}\right)}} = \\ &= 252.48220 \text{ rad/m} \quad , \\ \alpha_3 &= \frac{k_0}{\sqrt{2}}\sqrt{-1+\sqrt{1+\left(\frac{2\varepsilon''_{r2}}{\sin(2\xi_3)}\right)}} = \\ &= 12.5927 \text{ rad/m} \quad , \\ \frac{\beta_3}{k_0} &= \frac{252.48220}{252.167972} = 1.00125 \quad . \end{aligned} \tag{11}$$

Again, PEC was used for the horn structure, and PML was chosen for the boundary conditions of the simulation domain. A two-dimensional map of the electric field generated in a vacuum by the considered structure is shown in Fig. 16. Here, we can clearly see the effect of diffraction of the electromagnetic wave caused by the prism's wedge, because the prism is not much larger than the wave front as hypothesized in [6].

The amplitude of the phase vector β_3 was evaluated on Comsol, based on the assumption that the generated wave was inhomogeneous. From such a hypothesis, it follows:

$$E_y(x) = E_0 \mathrm{e}^{-\mathrm{j}\mathbf{k}_3\cdot\mathbf{r}} = E_0 \mathrm{e}^{-\mathrm{j}\beta_x x}\mathrm{e}^{-\boldsymbol{\alpha}\cdot\mathbf{r}} \tag{12}$$

so,

$$\ln E_y(x) = \ln E_0 - \mathrm{j}\beta_x x - \boldsymbol{\alpha}\cdot\mathbf{r} \tag{13}$$

and, finally:

$$\mathrm{Im}\left[\ln E_y(x)\right] = \mathrm{Im}\left[\ln E_0\right] - \beta_x x \,. \tag{14}$$

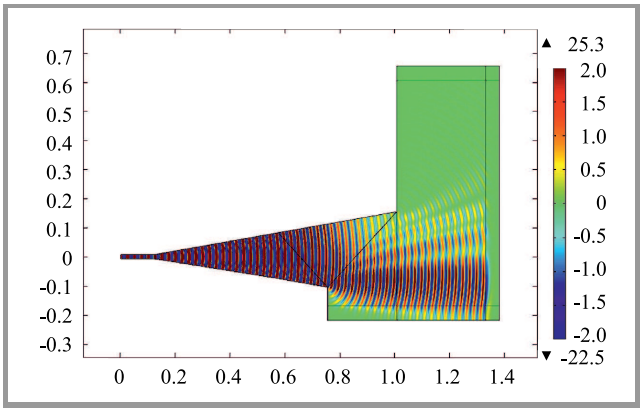

Fig. 16. Near-field radiation (V/m) of the horn lossy prism structure in vacuum: it can be observed that the radiation is directed normally to the separation interface. (See color pictures online at www.nit.eu/publications/journal-jtit)

Exporting some samples of the amplitude of the phase vector β_x in the direction normal to the lossy medium interface, and averaging the obtained values (as the phase vector amplitude presents a spatial periodicity), it was obtained $\beta_3/k_0 = 1.00119$. This value is in very good agreement with the one expected from [6], and it is only slightly lower, because the wave generated by this structure is not plane. After having confirmed that the lossy prism behaves as expected, we introduced the lossy medium already treated in the previous sections of this paper. The simulation results are shown in Fig. 17.

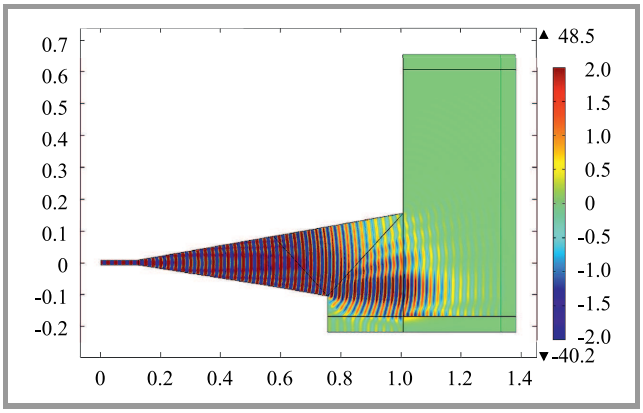

Fig. 17. Simulation of the horn-prism structure penetration on a lossy medium having unitary relative permittivity and permeability, and with conductivity $\sigma = 0.05$ S/m, the electric-field amplitude is expressed in V/m.

The amplitude of the field on the direction of maximum penetration was exported on Matlab and compared against

the penetration produced by the two-dimensional antenna presented in the previous paragraph. The result is displayed in Fig. 18.

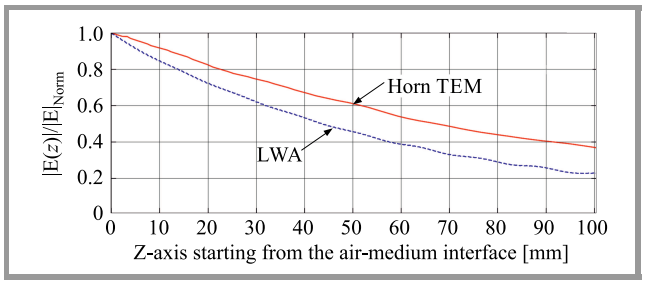

Fig. 18. Normalized electric-field amplitudes of horn-prism structure and two-dimensional leaky-wave antenna inside a non-magnetic lossy medium, with relative permittivity $\varepsilon_r = 1$ and conductivity $\sigma = 0.05$ S/m – Eq. (8).

The horn-prism structure clearly presents higher penetration, as predicted in [6]. This comes at the cost of loss of energy that gets dissipated inside the prism.

The base of the prism considered in this paper is as large as the two-dimensional TEM-horn antenna aperture. This choice reduces the losses in the prism to a minimum, but it is not ideal, because the theory was developed for an infinite long prism. We need therefore to confirm that the choice made does not compromise the expected behavior. Let us enlarge the base of the two-dimensional lossy prism, obtaining the antenna shown in Fig. 19.

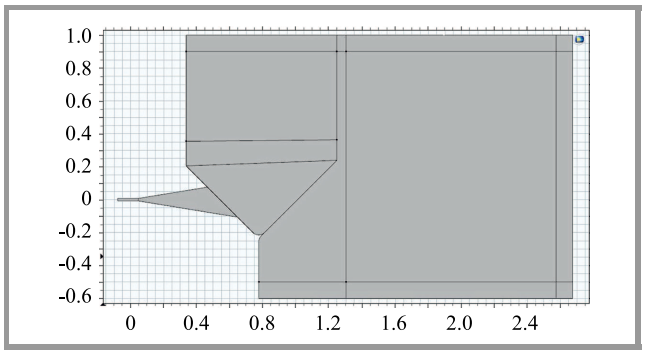

Fig. 19. Comsol simulation of a two-dimensional TEM-horn antenna device with lossy prism dimensions larger than the TEM-horn antenna aperture dimensions.

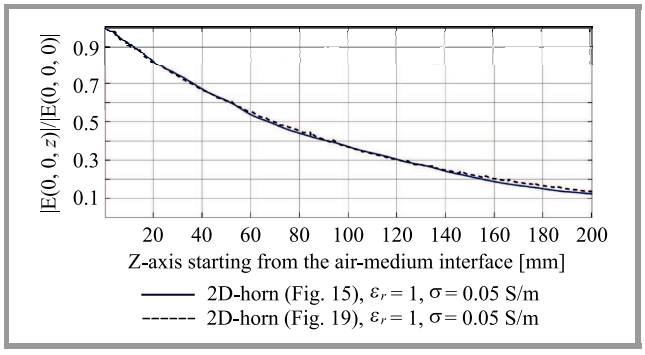

Fig. 20. Normalized electric-field amplitude achieved by employing the antenna illustrated in Fig. 19 compared with the one obtained by the antenna of Fig. 15 on a non-magnetic lossy medium, having relative permittivity $\varepsilon_r = 1$ and conductivity $\sigma = 0.05$ S/m – Eq. (8).

Let us, again, try to penetrate the lossy medium of unitary relative permittivity and conductivity of 0.05 S/m. The result of the comparison is available in Fig. 20. The two prisms show almost identical behavior: that is expected, noting that the original prism phase vector amplitude differs from the ideal one only by 6 ppm.

7. Lossy Prism Penetration on Realistic Media

A fundamental task is the evaluation of the penetration produced by the two-dimensional lossy prism on media having non-unitary permittivity, and in particular on media that can be encountered in realistic applications such as Ground Penetrating Radar (GPR). To perform such a task, we will consider clay, whose relative permittivity varies from 2 to 4, and conductivity varies depending on the humidity from 10^{-7} S/m (extremely dry clay), up to 10^{-1} S/m (extremely wet clay). We will consider here three samples having relative permittivity $\varepsilon_r = 3$ and conductivity $\sigma = 10^{-7}$ S/m, $\sigma = 10^{-5}$ S/m, and, finally, $\sigma = 10^{-3}$ S/m. We are going to predict analytically the expected penetration-curve behavior and then we will illustrate numerical simulations that will compare the penetration achieved by the lossy prism to the one achieved employing the customary horn antenna shown in Fig. 10.

7.1. Analytical Expectations for the Ideal Lossy Prism

The curve describing the amplitude of the electric field inside the lossy medium considered in the previous section does not resemble a horizontal line, as one would expect in the case of a deep-penetration condition (see Fig. 18). Let us analyze the reasons for this behavior approximating, again, the field produced by the lossy prism with a single inhomogeneous plane wave. Let us consider an inhomogeneous wave impinging normally on the separation surface with a lossy medium: with reference to Fig. 1, it is: $\xi_1 = \xi_2 = 0$, $\zeta_1 = 90°$, $0 < \zeta_2 < 90°$. It is then possible to evaluate the amplitude of the angle ζ_2 by knowing the amplitude of the attenuation vector of the incident wave through the generalized Snell laws and the separability conditions:

$$\begin{cases} \beta_2^2 - \alpha_2^2 = \mathrm{Re}\, k_2^2 \\ 2\beta_2\alpha_2 \cos(\zeta_2 - \xi_2) = 2\beta_2\alpha_2 \cos\zeta_2 = \mathrm{Im}\, k_2^2 \\ \alpha_2^2 \sin^2\zeta_2 = \alpha_1^2 \end{cases} . \quad (15)$$

Employing simple algebraic manipulations, we can write:

$$\begin{cases} 4\left(\mathrm{Re}\, k_2^2 + \alpha_2^2\right)\cdot\alpha_2^2\left(1 - \sin^2\zeta_2\right) = \mathrm{Im}^2 k_2^2 \\ \alpha_2^2 \sin^2\zeta_2 = \alpha_1^2 \end{cases} . \quad (16)$$

Now, setting $\sin^2\zeta_2 = \chi$ and substituting the second in the first of (16), a second-order equation in χ is obtained:

$$\left(\mathrm{Re}\,k_2^2\chi + \alpha_1^2\right)(1-\chi) = \frac{\mathrm{Im}^2 k_2^2}{4\alpha_1^2}\chi^2 \Rightarrow$$

$$\left(\mathrm{Re}\,k_2^2 + \frac{\mathrm{Im}^2 k_2^2}{4\alpha_1^2}\right)\chi^2 + \left(\alpha_1^2 - \mathrm{Re}\,k_2^2\right)\chi - \alpha_1^2 = 0\,.$$

We assumed a working frequency of $f_0 = 12$ GHz and we designed a lossy prism such that $\alpha_1 = 12.5927$ rad/m, see Eq. (11). For the medium considered in the previous paragraph $\sigma = 0.05$ S/m, $\mu_r = 1$, and $\varepsilon_r = 1$. In that case Eq. (17) predicts $\zeta_2 \approx 53.26°$. The component of the attenuation vector along the z axis is, in this case, not negligible with respect to the component along the interface. If, instead, $\mu_r = 1$, $\varepsilon_r = 3$, and $\sigma = 10^{-7}$ S/m are assumed in Eq. (17), we obtain $\zeta_2 \approx 89.9999°$. In this scenario the lossy prism approximates very well the "deep-penetration condition" and therefore it would penetrate almost indefinitely inside the lossy medium. The field inside the medium approximates a line parallel to the z axis because the component of $\boldsymbol{\alpha}$ along the z axis and responsible for the exponential attenuation inside the lossy medium is, in this case, negligible. When $\mu_r = 1$, $\varepsilon_r = 3$, and $\sigma = 10^{-3}$ S/m are considered, $\zeta_2 \approx 89.5°$. Also in this case, the curve describing the penetration should still be approximated as a line in the interval taken in this simulation (about 100 mm). In all considered cases the prism is expected to penetrate inside the lossy medium more deeply than the pyramidal horn.

7.2. Numerical Results

Let us now take the antenna shown in Fig. 19 and let us apply it to the three different configurations of clay considered. The penetration is, again, evaluated through the expression given in Eq. (8), and results are compared against the ones obtained by employing the customary pyramidal-horn antenna of Fig. 10. Results of the comparisons for the three media are shown in Figs. 21, 22, and 23, respectively. As expected, the field generated by the horn antenna decreases exponentially in the direction normal to the separation surface (it must be $\zeta_2 = 0$ in Fig. 1), while the field produced by the TEM-horn antenna equipped with the lossy prism presents a slope that, in the interval taken, resembles a line. The attenuation produced by the lossy medium on the inhomogeneous field generated is almost in perfect agreement with the value expected by Eq. (17) when $\sigma = 0.05$ S/m and $\varepsilon_r = 1$, but in the cases shown in Figs. 21–23, in which the conductivity has a lower amplitude, the attenuation produced on the field generated by the TEM-horn antenna is found to be slightly larger than the one predicted for the plane-wave. The attenuation on the wave due to the finite nature of the source is predominant in this case on the attenuation introduced by the lossy medium.

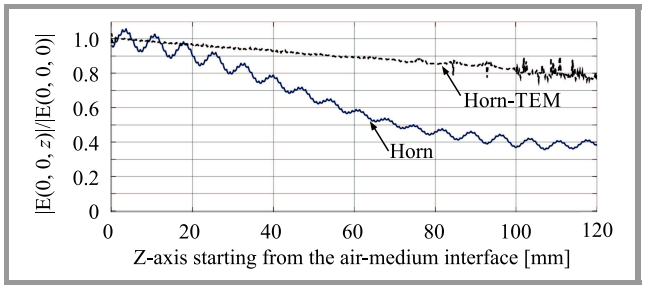

Fig. 21. Amplitudes of normalized electric fields generated by the lossy-prism antenna (dashed line) and a customary horn antenna evaluated inside a non-magnetic lossy medium having permittivity $\varepsilon_r = 3$ and conductivity $\sigma = 10^{-7}$ S/m in the direction normal to the separation interface and normalized by the field at the separation interface – Eq. (8).

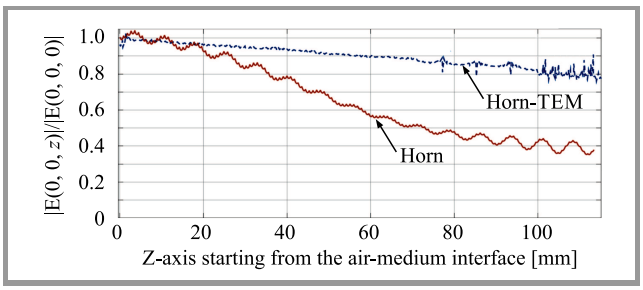

Fig. 22. Amplitudes of normalized electric fields generated by the lossy-prism antenna (dashed line) and a customary horn antenna evaluated inside a non-magnetic lossy medium having permittivity $\varepsilon_r = 3$ and conductivity $\sigma = 10^{-5}$ S/m in the direction normal to the separation interface and normalized by the field at the separation interface – Eq. (8).

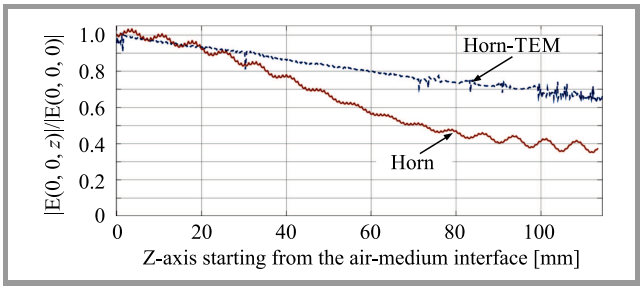

Fig. 23. Amplitudes of normalized electric fields generated by the lossy-prism antenna (dashed line) and a customary horn antenna evaluated inside a non-magnetic lossy medium having permittivity $\varepsilon_r = 3$ and conductivity $\sigma = 10^{-3}$ S/m in the direction normal to the separation interface and normalized by the field at the separation interface – Eq. (8).

8. Conclusions

In this paper, a larger penetration achievable by inhomogeneous waves was investigated numerically by simulating common horn antennas and inhomogeneous-wave generators. Attention was paid to broadside radiation, which represents a common requirement for many practical applications, highlighting that the inhomogeneous radiation may be not only a necessary condition, but also a sufficient condi-

tion for achieving penetration larger than the one achievable by commonly used and more traditional antenna geometries. It was verified, at least for the numerical scenarios considered, that the closer the losses in the medium get to the condition of deep-penetration, the higher the difference in penetration between homogeneous and inhomogeneous waves. It was also verified that the expectation that higher penetration is achieved increasing the incidence angle is confirmed by numerical simulations employing realistic waveforms and not only by the former analytical plane-wave demonstrations, as done in previous works presented in the literature. Finally, we concentrated on the recently proposed geometry of the lossy prism structure, showing that, where losses in the prism are an acceptable compromise, this structure can guarantee deeper penetration than the one obtainable through other leaky-wave antennas presented in the literature [3]. The deep penetration employing a lossy prism comes at the price of dissipation of energy in form of heating, so, the energy available at the separation interface between lossless and lossy media is lower than the one produced by the feeding antenna, this may be suitable only in certain scenarios, as discussed in the paper.

9. Future work

The simulations exposed in this paper show encouraging results but they are still early-stage outcomes that will need to be confirmed by operating a larger number of comparisons. A more realistic tapered TEM antenna, such as the one presented in [27], should be considered. Moreover, the results given here are valid for a single frequency, while the impact on UWB applications and antennas should also be evaluated. Further simulations will have to be performed to demonstrate the suitability of this structure to interesting scenarios such as hyperthermia or Ground Penetrating Radar. Those simulations could require a re-design and further optimization of the antenna proposed here. Moreover, penetration is only one factor to be evaluated in antenna design, realistic applications will need also to consider important characteristics such as phase-center stability and bandwidth.

Acknowledgements

The authors are deeply indebted to the GPR COST Action TU1208 and its network activities that made this study possible.

References

[1] F. Frezza and N. Tedeschi, "Deeply penetrating waves in lossy media", *Optics Letters*, vol. 37, no. 13, pp. 2616–2618, 2012 (doi: 10.1364/OL.37.002616).

[2] F. Frezza and N. Tedeschi, "On the electromagnetic power transmission between two lossy media: discussion", *J. of the Opt. Soc. of America A*, vol. 29, no. 11, pp. 2281–2288, 2012 (doi:10.1364/JOSAA.29.002281).

[3] A. A. Oliner and D. R. Jackson, "Leaky-Wave Antennas", in *Antenna Engineering Handbook*, 4th Edition, Chap. 11, John Volakis Editor, McGraw Hill Professional, 2007.

[4] D. R. Jackson and A. A. Oliner, "Leaky-wave antennas", in *Modern Antenna Handbook* (C. A. Balanis, Ed.), pp. 325-367, New York: Wiley, 2008.

[5] P. Baccarelli, F. Frezza, P. Simeoni, and N. Tedeschi, "Inhomogeneous Wave Penetration in Lossy Media", in *Proc. Int. Symp. on EM Theory EMTS 2016*, Espoo, Finland, 2016 (doi: 10.1109/URSI-EMTS.2016.2016.7571523).

[6] F. Frezza, P. Simeoni, and N. Tedeschi, "Analytical Investigation on a New Approach for achieving Deep Penetration in a Lossy medium: the Lossy Prism", *J. of Telecommun. and Infor. Technol.*, no. 3, pp. 17–24, 2017 (doi: 10.26636/jtit.2017.119917).

[7] F. Frezza, *A Primer on Electromagnetic Fields*. Springer, 2015.

[8] F. Frezza and N. Tedeschi, "Electromagnetic inhomogeneous waves at planar boundaries: tutorial", *J. of the Opt. Soc. of America A*, vol. 32, no. 8, pp. 1485–1501, 2015 (doi: 10.26636/jtit.2017.119917).

[9] F. Frezza, S. Leo, F. Mangini, N. Tedeschi, and P. Simeoni, "Deep Penetration in Lossy Media Through Non Uniform Electromagnetic Waves", in *Proc. the Third TU1208 Action Gen. Meeting*, London, United Kingdom, 2015, Aracne.

[10] T. Zhao, D. R. Jackson, J. T. Williams, H. Y. D. Yang, and A. A. Oliner, "2-D Periodic Leaky-Wave Antennas-Part I: Metal Patch Design", *IEEE Transact. on Antennas and Propag.*, vol. 53, no. 11 pp. 3505–3514, 2005 (doi: 10.1109/TAP.2005.858579).

[11] N. G. Alexopoulos and D.R. Jackson, "Fundamental superstrate (cover) effects on printed circuit antennas", *IEEE Transact. on Antennas and Propag.*, vol. AP-32, pp. 807–816, 1984 (doi: 10.1109/TAP.1984.1143433).

[12] D. R. Jackson and N. G. Alexopoulos, "Gain Enhancement method for Printed Circuit Antennas", *IEEE Transact. on Antennas and Propag.*, vol. AP-33, pp. 976–987, 1985.

[13] M. Ettore, "Analysis and design of efficient planar leaky-wave antennas", Ph. D. Thesis, University of Siena, 2008.

[14] P. Burghignoli, G. Lovat, and D. R. Jackson, "Analysis and optimization of leaky-wave radiation at broadside from a class of 1-D periodic structures", *IEEE Transact. on Antennas and Propag.*, vol. 54, no. 9, pp. 2593–2604, 2006 (doi: 10.1109/TAP.2006.880725).

[15] S. Paulotto, P. Baccarelli, F. Frezza, and D. R. Jackson, "A novel technique for open-stopband suppression in 1-D periodic printed leaky-wave antennas", *IEEE Transactions on Antennas and Propagation*, vol. 57, no. 7, pp. 1894-1906, 2009 (doi: 10.1109/TAP.2009.2019900).

[16] CST Microwave Studio, "Version 2014", Darmstadt (Germany), CST GmbH, 2014.

[17] T. Zhao, D. R. Jackson, J. T. Williams, and A. A. Oliner, "General formulas for 2-D leaky-wave antennas", *IEEE Transact. on Antennas and Propag.*, vol. 53, no. 11, pp. 3525–3533, 2005 (doi: 10.1109/TAP.2005.856315).

[18] R. Garg, *Microstrip antenna design handbook*, Boston, MA: Artech House, 2001.

[19] F. Frezza and N. Tedeschi, "Total transmission of inhomogeneous electromagnetic waves at planar interfaces", *Phys. Rev. A*, vol. 92, 053853, 2015 (doi: 10.1103/PhysRevA.92.053853).

[20] C. A. Balanis, *Antenna theory: analysis and design,* New York: Wiley, 2016.

[21] CST, "Workflow Example Horn Antenna", *CST Microwave Studio Training Class*, 2009.

[22] W. Menzel, "A new travelling-wave antenna in microstrip", in *Proc. 8th Eur. Microwave Conf.*, Paris, France, 1978, pp. 302–306 (doi: 10.1109/EUMA.1978.332503).

[23] A. A. Oliner and K. S. Lee, "Microstrip leaky wave strip antennas", in *Proc. IEEE Int. Symp. on Antennas and Propag.*, Philadelphia, PA, USA, 1986, pp. 443–446 (doi: 10.1109/APS.1986.1149629).

[24] N. Tedeschi and F. Frezza, "An analysis of the inhomogeneous wave interaction with plane interfaces", in *Proc. Gen. Ass. and Scient. Symp. URSI GASS*, Beijing, China, 2014, pp. 109–112 (doi: 10.1109/URSIGASS.2014.6929097).

[25] N. Tedeschi, V. Pascale, F. Pelorossi, and F. Frezza, "Generation of inhomogeneous electromagnetic waves by a lossy prism", in *Proc. Int. Symp. on EM Theory EMTS 2016*, Espoo, Finland, 2016 (doi: 10.1109/URSI-EMTS.2016.7571534).

[26] S. A. Schelkunoff and H. T. Friis, *Antennas Theory and Practice*, New York: Wiley, 1952.
[27] S. Bassam and J. Rashed-Mohassel, "A Chebyshev tapered TEM horn antenna", *PIERS Online*, vol. 2, no. 6, pp. 706–709, 2016 (doi: 10.2529/PIERS060902041831).

Alessandro Calcaterra received his B.Sc. and M.Sc. degrees in Electronic Engineering with full marks and honors, both from the University of Rome "La Sapienza" in 2014 and 2017, respectively. During his academic career he attended two different advanced courses, in which he could deeply improve his knowledge on the electromagnetic theory, on the characteristics of materials at microwave frequencies and on leaky-wave antennas. In particular, the latter represents his main topic of interest that he could enhance by attending the ESoA course on "Leaky-waves and periodic structures for antenna applications" in 2017. At the moment, he is enrolled in the Ph.D. course in Electromagnetism at the University of Rome "La Sapienza", studying the deep-penetration phenomenon and how to achieve it using inhomogeneous waves such as leaky ones.

E-mail: alessandro.calcaterra@uniroma1.it
Department of Information Engineering, Electronics and Telecommunications
La Sapienza University of Rome
via Eudossiana 18
00184 Rome, Italy

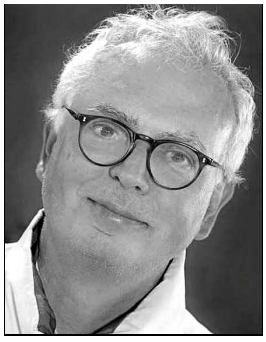

Fabrizio Frezza received the "Laurea" degree (cum laude) in Electronics Engineering and the Ph.D. degree in Applied Electromagnetics and Electrophysical Sciences from La Sapienza University of Rome, Italy, in 1986 and 1991, respectively. He joined the Department of Electronics, Sapienza University of Rome, in 1986, where he was a Researcher from 1990 to 1998, a Temporary Professor of Electromagnetic Fields from 1994 to 1998, and an Associate Professor from 1998 to 2004. He has been a Full Professor of Electromagnetic Fields with Sapienza University of Rome since 2005. His current research interests include guiding structures, antennas and resonators for microwaves and millimeter waves, numerical methods, scattering, optical propagation, plasma heating, anisotropic media, artificial materials, and metamaterials.

E-mail: fabrizio.frezza@uniroma1.it
Department of Information Engineering, Electronics and Telecommunications
La Sapienza University of Rome
via Eudossiana 18
00184 Rome, Italy

Patrizio Simeoni received both the "Laurea" (degree) in Electronic Engineering and the Ph.D. in Mathematical Models for Engineering, Electromagnetics and Nanosciences from "La Sapienza" University of Rome, Italy. He worked as an embedded, software and system engineer from 2002. As a software engineer, he developed firmware on both DSPs and controllers, device drivers and user-level applications. As a system engineer he collaborated in the design of solutions for telecommunication and transport projects. His main research topic in electromagnetism is the study of electromagnetic-wave penetration in lossy media. Since 2012, he has been employed in the National Transport Authority, Ireland, as a senior technical engineer in the Integrated Ticketing System project.

E-mail: patrizio.simeoni@nationaltransport.ie
National Transport Authority (NTA)
Dún Scéine
Harcourt Lane
Dublin 2
Dublin, Ireland

Nicola Tedeschi received the M.Sc. degree in Electronic Engineering and the Ph.D. degree from La Sapienza University of Rome, Rome, Italy, in 2009 and 2013, respectively. Currently, he is a Postdoctoral Fellow with La Sapienza University of Rome. He was a visiting student with the Department of Radio Science and Engineering, Aalto University, Espoo, Finland, in 2012. His research interests include electromagnetic scattering by objects near interfaces, propagation of inhomogeneous waves in dissipative media, and characterization of dispersive properties of natural and artificial materials.

E-mail: nicola.tedeschi@uniroma1.it
Department of Information Engineering, Electronics and Telecommunications
La Sapienza University of Rome
via Eudossiana 18
00184 Rome, Italy